ACS APPLIED MATERIALS & INTERFACES

www.acsami.org

Research Article

Reactive Chlorine Capture by Dichlorination of Alkene Linkers in Metal−Organic Frameworks

Tyler J. Azbell,[§] Ruth M. Mandel,[§] Jung-Hoon Lee, and Phillip J. Milner*

Cite This: *ACS Appl. Mater. Interfaces* 2022, 14, 53928−53935

Read Online

ACCESS | Metrics & More | Article Recommendations | Supporting Information

ABSTRACT: Chlorine (Cl_2) is a toxic and corrosive gas that is both an essential reagent in industry and a potent chemical warfare agent. Materials that can strongly bind Cl_2 at low pressures are essential for industrial and civilian personal protective equipment (PPE). Herein, we report the first examples of irreversible Cl_2 capture via the dichlorination of alkene linkages in Zr-based metal−organic frameworks. Frameworks constructed from fumarate (Zr-fum) and stilbene (Zr-stilbene) linkers retain long-range order and accessible porosity after alkene dichlorination. In addition, energy-dispersive X-ray spectroscopy reveals an even distribution of Cl throughout both materials after Cl_2 capture. Cl_2 uptake experiments reveal high irreversible uptake of Cl_2 (>10 wt %) at low partial pressures (<100 mbar), particularly in Zr-fum. In contrast, traditional porous carbons mostly display reversible Cl_2 capture, representing a continued risk to users after exposure. Overall, our results support that alkene dichlorination represents a new pathway for reactive Cl_2 capture, opening new opportunities for binding this gas irreversibly in PPE.

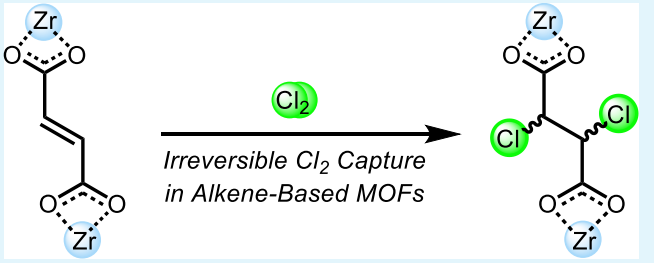

KEYWORDS: *chlorination, metal−organic framework, chemisorption, personal protective equipment, porosity*

INTRODUCTION

Chlorine (Cl_2) is an essential reagent in the polymer, pharmaceutical, and agrochemical industries and is widely employed for water sanitation as well.[1] Unfortunately, Cl_2 is also a corrosive and toxic gas that has been historically used as a chemical warfare agent. Indeed, Cl_2 exposure can result in immediate injury or death, and even brief exposure (1−3 ppm in air under an hour) can be fatal.[2] Due to its ubiquity, Cl_2 poses a serious hazard across many industries.[1] Industrial Cl_2 sequestration is typically carried out using aqueous caustic soap solutions, which are not amenable to garment-based personal protective equipment (PPE).[1,3] Adding to its immediate threat to human safety, Cl_2 also decomposes into ozone layer degradants upon release into the environment.[4−6] As such, there is an urgent need to develop new solid materials capable of strongly binding Cl_2 before it can cause personal or environmental harm.

Irreversible sequestration in porous solids would provide improved protection from Cl_2 compared to reversible binding via weak physisorption. However, the highly corrosive nature of Cl_2 makes its selective capture a challenge.[5,7] Porous carbons have been previously employed to reversibly sequester gaseous Cl_2, but their lack of structural tunability makes the introduction of irreversible Cl_2-reactive sites difficult.[8] Additionally, the dichlorination of olefin-containing polymers has been employed to generate novel chlorinated polymers, but there are few examples that do not suffer from degradation due to over-chlorination.[9,10] Metal−organic frameworks (MOFs) are crystalline, porous materials assembled from organic linkers and inorganic nodes that are amenable to applications relevant to corrosive gas handling, including their storage, neutralization, and sensing.[11−16] Reactive capture in MOFs via post-synthetic modification is an appealing means to employ MOFs for low-pressure halogen binding.[17,18] In addition, the rapid diffusion of Cl_2 through MOF pores and accessibility to all of the alkene linkages make them ideal candidates for irreversible Cl_2 capture compared to non-porous polymers. However, examples of MOFs that retain their crystallinity and accessible porosity after direct exposure to elemental halogens, especially Cl_2 and bromine (Br_2), remain relatively rare.[13,17−25] For example, exposure of the MOF NH_2-UiO-66 (UiO = Universitetet i Oslo) to Cl_2 was previously reported to result in a substantial loss in framework crystallinity due to uncontrolled electrophilic aromatic substitution.[16,19,26]

We hypothesized that dichlorination of alkene linkages in MOFs would represent a new, reactivity-based pathway for irreversible Cl_2 capture in porous materials. Among MOFs, those assembled from Zr(IV) secondary building units, known as Zr-MOFs, demonstrate a high degree of chemical

Received: October 5, 2022
Accepted: November 9, 2022
Published: November 22, 2022

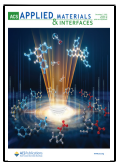

https://doi.org/10.1021/acsami.2c17966
ACS Appl. Mater. Interfaces 2022, 14, 53928−53935

Scheme 1. Structures of the Frameworks Studied in This Work; Cl_2−Zr-Fum (a) and Cl_2−Zr-Stilbene (b) were Obtained through Post-Synthetic Chlorination of the Starting Frameworks Zr-Fum and Zr-Stilbene, Respectively[a]

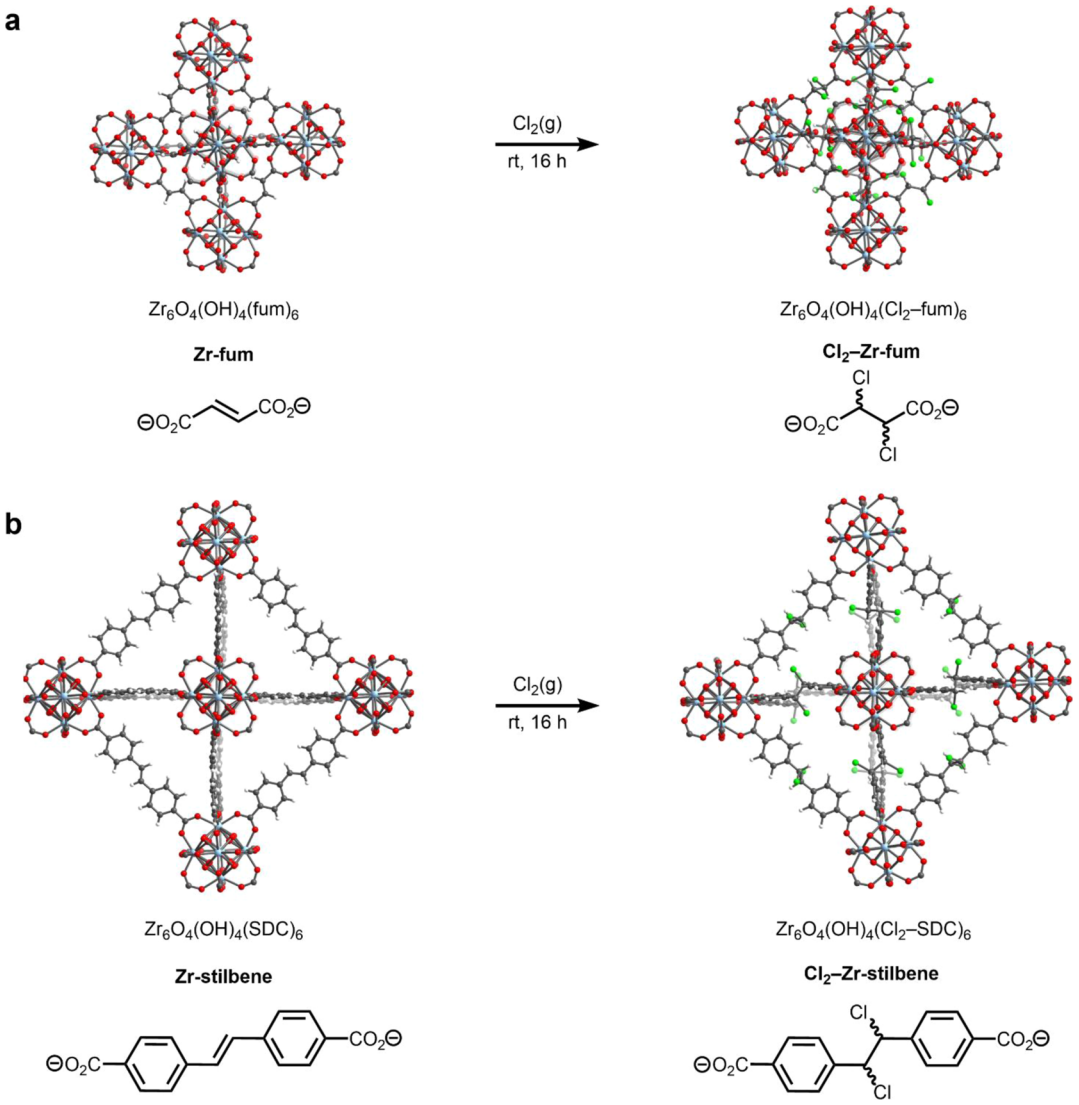

[a]Gray, green, red, white, and sky-blue spheres correspond to carbon, chlorine, oxygen, hydrogen, and zirconium, respectively.

robustness, including toward corrosive gases.[26−30] Indeed, bromination and iodination of alkenes within Zr- and analogous Hf-based MOFs have been previously demonstrated[17,18,31] and support the feasibility of halogen capture in alkene-containing MOFs. However, given the significantly higher reactivity of Cl_2 compared to Br_2 and iodine (I_2), prior to our work, it remained unclear whether MOFs could undergo linker dichlorination without complete framework degradation.

Herein, we report the first examples of direct alkene dichlorination in MOFs, specifically in the Zr-MOFs $Zr_6O_4(OH)_4(fum)_6$ (fum^{2-} = fumarate), known as MOF-801 or Zr-fum, and $Zr_6O_4(OH)_4(SDC)_6$ (SDC^{2-} = 4,4′-(ethene-1,2-diyl)dibenzoate), also known as Zr-stilbene. Upon exposure to Cl_2 gas, both MOFs retain crystallinity and porosity while undergoing high degrees of linker dichlorination. Additionally, these MOFs irreversibly capture Cl_2 at low pressures, making them potentially suitable for grafting to fabric for PPE.[13] Overall, our findings add linker dichlorination to the lexicon of strategies available for irreversible Cl_2 capture in porous materials.

RESULTS AND DISCUSSION

We began our investigation into Cl_2 capture by alkene dichlorination using Zr-fum as a representative alkene-containing MOF (Scheme 1). This framework is constructed from Zr_6 nodes bridged by fumarate (fum^{2-}) linkers, resulting in a microporous material with an overall face-centered cubic fcu topology.[32] Like other Zr-based MOFs, the strong Zr−O bonds in this framework lend it remarkable chemical stability toward ambient air, water, and corrosive gases.[28,33] In addition, Zr-fum possesses a high density of accessible alkene sites for potential dichlorination. Combined with its scalable synthesis from inexpensive, easily accessible materials, these properties make Zr-fum a promising candidate for irreversible Cl_2 capture. Following the literature procedure,[34] Zr-fum was synthesized on an ∼18 g scale, as confirmed by powder X-ray diffraction (PXRD) and surface area analysis (Figure 1a,b, see Supporting Information Section 2 for details).

The ability of Zr-fum to irreversibly capture Cl_2 was assessed by exposing the MOF to <100 mbar of Cl_2 diluted in N_2 for 16 h, producing what we refer to herein as Cl_2−Zr-fum (see

https://doi.org/10.1021/acsami.2c17966
ACS Appl. Mater. Interfaces 2022, 14, 53928−53935

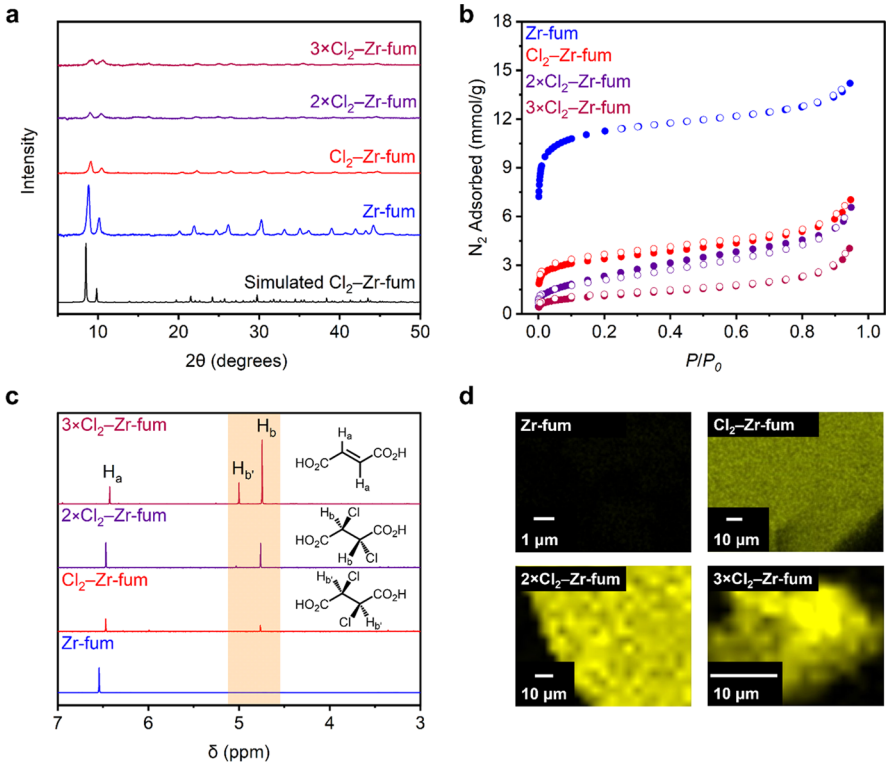

Figure 1. (a) PXRD patterns (λ = 1.5406 Å) of Zr-fum (blue), Cl_2–Zr-fum (red), 2 × Cl_2–Zr-fum (purple), and 3 × Cl_2–Zr-fum (maroon). The simulated pattern based on the previously reported single-crystal X-ray diffraction structure of Zr-fum is included for reference. (b) 77 K N_2 adsorption (filled) and desorption (open) isotherms of Zr-fum (blue), Cl_2–Zr-fum (red), 2 × Cl_2–Zr-fum (purple), and 3 × Cl_2–Zr-fum (maroon). (c) Digestion ^{1}H NMR (400 MHz, DMSO-d_6) spectra of Zr-fum (blue), Cl_2–Zr-fum (red), 2 × Cl_2–Zr-fum (purple), and 3 × Cl_2–Zr-fum (maroon), with the orange highlighted region indicating the gradual appearance of two new diastereomeric aliphatic C–H protons as more of the starting fumarate linker is chlorinated. (d) Cl EDS maps of Zr-fum (top left), Cl_2–Zr-fum (top right), 2 × Cl_2–Zr-fum (bottom left), and 3 × Cl_2–Zr-fum (bottom right).

Supporting Information Section 3 for details). Remarkably, even after direct exposure to Cl_2 gas, the MOF retained modest crystallinity as measured by PXRD without the appearance of any new reflections (Figure 1a, Supporting Information Figure S11). This is comparable to NH_2-UiO-66, which was previously reported to lose significant crystallinity under similar conditions.[19] Scanning electron microscopy (SEM) analysis of Cl_2–Zr-fum revealed a lack of well-defined surface morphology compared to the starting spherical-shaped Zr-fum crystallites (Supporting Information Figures S7 and S17), consistent with the partial loss of long-range order after Cl_2 exposure. Nonetheless, after activation under high vacuum to remove any physisorbed Cl_2 gas, 77 K N_2 sorption analysis revealed that Cl_2–Zr-fum is still permanently porous, with a Brunauer–Emmett–Teller (BET) surface area of 276 ± 1 m^2/g (Figure 1b, Supporting Information Figure S13). This significant reduction in surface area compared to the starting framework (BET surface area of 970 ± 2 m^2/g) coupled with the retention of crystallinity by PXRD is consistent with the reactive capture of Cl_2 via addition across the alkene double bonds, along with some partial degradation.

To interrogate whether linker dichlorination occurs in the MOF upon exposure to Cl_2, Cl_2–Zr-fum was characterized by ^{1}H NMR after acidic digestion, combustion elemental analysis, and energy-dispersive X-ray spectroscopy (EDS) (Figure 1c,d). After digestion, ^{1}H NMR revealed the presence of a new resonance at δ 4.77 ppm in Cl_2–Zr-fum that is absent in Zr-fum, which is assigned to a proton adjacent to the newly formed C–Cl bond (Figure 1c, Supporting Information Figure S15). Assuming chloronium ion formation is favored, we assign this species as the *anti*-diastereomer (see below for discussion). However, the starting fumarate linker was also observed (δ 6.47 ppm). Integrating these two peaks afforded a 1:0.57 ratio of the starting linker to the dichlorinated linker, indicating that approximately 36% of the fumarate linkers reacted with Cl_2. Given the small pores of Zr-fum (5–7 Å),[32] it is unsurprising that incomplete linker dichlorination occurs under these conditions. Importantly, EDS confirmed the permanent presence of Cl in Cl_2–Zr-fum (Figure 1d, Supporting Information Figure S19) that is absent in Zr-fum (Figure 1d, Supporting Information Figure S9). However, an over-abundance of Cl in Cl_2–Zr-fum was detected by EDS (21.8 atomic %) compared to the theoretical value, assuming ~36% linker dichlorination (10.2 atomic %, Supporting Information Table S3). As EDS is a surface-sensitive technique, this finding implies that the reaction of linkers with Cl_2 likely occurs mostly on the surface of MOF crystallites, hindering further reaction within the pores. Consistently, combustion analysis provided a closer match between the experimental (15.1 wt %) and theoretical (10.1 wt %) % Cl values in Cl_2–Zr-fum (Supporting Information Table S4). Overall, these data unequivocally support that the fumarate linkers of Zr-fum can be dichlorinated directly using Cl_2.

We hypothesized that repeatedly exposing Cl_2–Zr-fum to Cl_2 should lead to increased linker dichlorination. After a second and third exposure to Cl_2, the resulting frameworks, herein referred to as 2 × Cl_2–Zr-fum and 3 × Cl_2–Zr-fum, respectively, both exhibited dramatic reductions in crystallinity

https://doi.org/10.1021/acsami.2c17966
ACS Appl. Mater. Interfaces 2022, 14, 53928–53935

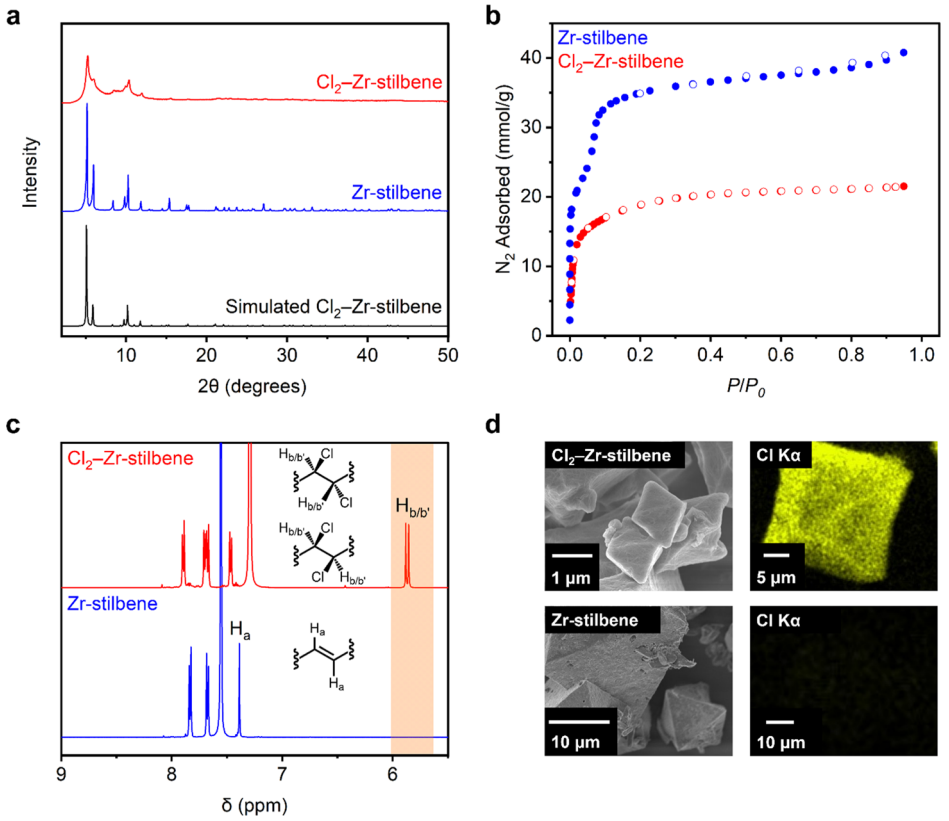

Figure 2. (a) PXRD patterns (λ = 1.5406 Å) of Zr-stilbene (blue) and Cl_2−Zr-stilbene (red). The simulated pattern based on the previously reported single-crystal X-ray diffraction structure of Zr-stilbene is included for reference. (b) 77 K N_2 adsorption (filled) and desorption (open) isotherms of Zr-stilbene (blue) and Cl_2−Zr-stilbene (red). (c) Digestion ^{1}H NMR (400 MHz, DMSO-d_6) spectra of Zr-stilbene (blue) and Cl_2−Zr-stilbene (red), with the orange highlighted region indicating the appearance of two new diastereomeric aliphatic C−H protons in the latter material. (d) SEM images and the corresponding Cl EDS maps of Cl_2−Zr-stilbene (top) and Zr-stilbene (bottom).

by PXRD (Figure 1a, Supporting Information Figures S20 and S29). A concomitant decrease in BET surface areas upon repeated Cl_2 exposure was also observed from 276 ± 1 m^2/g in Cl_2−Zr-fum to 186 ± 3 m^2/g in 2 × Cl_2−Zr-fum and 87 ± 1 m^2/g in 3 × Cl_2−Zr-fum (Figure 1b, Supporting Information Figure S22). Consistently, repeated Cl_2 exposure led to an increase in the Cl_2−fum:fum ratio by ^{1}H NMR after digestion from 0.57:1 in Cl_2−Zr-fum to 1.06:1 in 2 × Cl_2−Zr-fum to 4.18:1 in 3 × Cl_2−Zr-fum (Figure 1c, Supporting Information Figures S25 and S26). A new resonance at δ 5.00 ppm emerged in the digestion NMR spectra of 2 × Cl_2−Zr-fum and 3 × Cl_2−Zr-fum as well. We assign this resonance to the *syn*-diastereoisomer resulting from competing *syn*-dichlorination of the fumarate linker through a carbocation intermediate.[34−36] This assignment is corroborated by the ^{1}H−^{13}C HSQC NMR spectrum of 3 × Cl_2−Zr-fum, which clearly shows three distinct species in the digestion mixture: two distinct dichlorinated diastereomeric linkers as well as the starting fumarate linker (Supporting Information Figure S28).

Taking into account the contribution of both the *syn*- and *anti*-diastereomers to the total chlorinated linker content, the chlorination percent calculated from NMR rose from approximately 36% in Cl_2−Zr-fum to 53% in 2 × Cl_2−Zr-fum to 85% in 3 × Cl_2−Zr-fum. While Cl was evenly distributed in both materials by elemental EDS mapping (Figure 1d, Supporting Information Figures S31 and S33), the calculated atomic % of Cl by EDS was lower than the theoretical atomic % for both samples (Supporting Information Tables S5 and S6), highlighting the unreliable nature of this technique for non-surface elemental quantification. Again, combustion elemental analysis proved to be more reliable, as the observed Cl wt % for 3 × Cl_2−Zr-fum (18.4%) is comparable to the theoretical value (21.0%, Supporting Information Table S7). Due to the near-amorphous and non-porous nature of 3 × Cl_2−Zr-fum, it is likely that complete chlorination of the fumarate linkers in this material is not possible as a result of pore clogging upon dichlorination. Consistently, attempts to chlorinate the related framework Zr-mes, which has even smaller pores than Zr-fum, led to incomplete linker dichlorination as well (see Supporting Information Section 7 for details).

In order to achieve full linker dichlorination in a Zr-MOF, we turned to Zr-stilbene, an isoreticularly expanded analogue of Zr-fum with ∼15 Å pores (Scheme 1).[37] This framework has been previously shown to undergo post-synthetic bromination with Br_2 in complete conversion.[17] We hypothesized that the inherent stability and larger pores of Zr-stilbene would enable its reaction with Cl_2 to cleanly furnish the fully chlorinated framework, referred to herein as Cl_2−Zr-stilbene. The synthesis of Zr-stilbene following the previously reported procedure[38] yielded this framework on ∼0.5 g scale, as confirmed by PXRD and surface area analysis (Figure 2a,b, see Supporting Information Section 4 for details). In contrast to Zr-fum, Zr-stilbene was obtained as well-defined octahedral crystallites approximately 20 μm across (Supporting Information Figure S41). The pore size distribution analysis of Zr-stilbene assuming a slit-pore geometry confirmed that it possesses accessible pores approximately 15 Å in diameter,

https://doi.org/10.1021/acsami.2c17966
ACS Appl. Mater. Interfaces 2022, 14, 53928−53935

large enough to facilitate diffusion of Cl_2 through the framework even after partial linker dichlorination (Supporting Information Figure S38).

Utilizing the same reaction setup employed for the dichlorination of Zr-fum, Zr-stilbene was exposed to ~100 mbar of Cl_2 diluted in N_2 for 16 h (see Supporting Information Section 5 for details). Although a significant decrease in crystallinity was observed, Cl_2−Zr-stilbene still retained modest crystallinity by PXRD (Figure 2a, Supporting Information Figure S44). In particular, no new reflections corresponding to impurities were observed. SEM analysis of Cl_2−Zr-stilbene revealed that the inherent octahedral morphology of the parent Zr-stilbene crystallites was maintained even after prolonged Cl_2 exposure (Figure 2d, Supporting Information Figures S41 and S51). The observed decrease in crystallinity coupled with the retention of morphology by SEM indicates that some of the loss in long-range order in Cl_2−Zr-stilbene may be due to the increased flexibility of newly formed sp^3-hybridized carbons in the framework backbone.[39,40] Like Zr-fum, Zr-stilbene exhibited a reduction in porosity after Cl_2 exposure, with the 77 K N_2 BET surface area dropping from 2910 ± 37 m^2/g in the parent framework to 1549 ± 4 m^2/g in Cl_2−Zr-stilbene (Figure 2b, Supporting Information Figure S46). Pore size distribution analysis confirmed that the pores of Cl_2−Zr-stilbene are slightly smaller in diameter on average (13 Å) than those of Zr-stilbene (15 Å), consistent with the introduction of large Cl atoms within the pores (Supporting Information Figure S48).

To support the successful dichlorination of the alkene linkers in Cl_2−Zr-stilbene, ^1H NMR analysis of the acid-digested MOF was carried out (Figure 2c, Supporting Information Figure S49). As expected, complete consumption of the starting alkene linker was observed, as confirmed by the disappearance of the alkene proton chemical shift at δ 7.39 ppm. Two sets of new resonances, corresponding to dichlorinated diastereomers, were observed approximately in a 1:1 ratio. The presence of two diastereomers was confirmed by ^1H−^{13}C HSQC NMR spectroscopy (Supporting Information Figure S53), which revealed that each of the two singlets at δ 5.86 and δ 5.88 ppm in the ^1H NMR spectrum couple to two different ^{13}C resonances at δ 64 and δ 66 ppm, as expected for chlorinated benzylic ^{13}C centers. This finding suggests that the dichlorination of Zr-stilbene was surprisingly non-stereospecific, yielding approximately equal amounts of the *syn*- and *anti*-dichlorinated diastereomers. Given that the alkene in Zr-stilbene is flanked by two aromatic rings, the gas−solid phase dichlorination reaction likely proceeds via a resonance-stabilized carbocation intermediate and not via a chloronium ion.[41] The divergent stereoselectivity observed for the dichlorination of Zr-fum (Figure 1c) and Zr-stilbene (Figure 2c) arises from the different nature of the alkenes in these materials: the electron-withdrawing carboxylate groups in Zr-fum likely disfavor carbocation formation, favoring dichlorination via a chloronium ion, whereas the aryl groups in Zr-stilbene facilitate carbocation formation, leading to erosion in diastereoselectivity.

Similar to Cl_2−Zr-fum, the EDS analysis of Cl_2−Zr-stilbene revealed an even distribution of Cl throughout the crystalline lattice (Figure 2d, Supporting Information Figure S56); these Cl atoms are not observed in the parent Zr-stilbene (Figure 2d, Supporting Information Figure S43). In addition, combustion elemental analysis revealed that the experimental Cl wt % of Cl_2−Zr-stilbene (15.3 wt %) is in remarkably good agreement with the theoretical value assuming 100% chlorination (15.7 wt %), confirming that clean alkene dichlorination occurs in this MOF (Supporting Information Table S11). It should be noted that ^1H NMR analysis also confirmed that Zr-stilbene did not undergo electrophilic aromatic substitution, indicating a high level of chemoselectivity for alkene dichlorination in this material.[42]

The results discussed above confirm that Zr-fum and Zr-stilbene were cleanly dichlorinated in the presence of Cl_2 gas while partially retaining their crystallinity and porosity. Building upon these findings, we evaluated their ability to rapidly and irreversibly capture Cl_2 at low partial pressures relevant to PPE.[2] Unfortunately, volumetric Cl_2 sorption isotherms would be uninformative due to the irreversible nature of Cl_2 uptake in these materials.[43] Therefore, gravimetric Cl_2 uptake measurements were carried out using a custom-built, stainless-steel manifold connected to a Cl_2 cylinder and a low-pressure manometer, which allowed for the delivery of progressively increasing volumes of Cl_2 to both MOFs (see Supporting Information Section 6 for details). After being exposed to Cl_2 for 20 min, both MOFs were degassed and re-weighed, allowing for the calculation of their irreversible gravimetric Cl_2 uptakes at each pressure of Cl_2 after short exposure times. The results of these experiments are included in Figure 3.

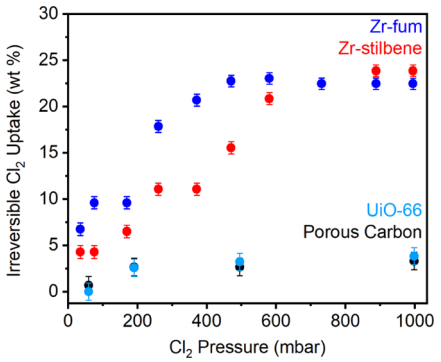

Figure 3. Irreversible Cl_2 uptake at different Cl_2 pressures for the MOFs Zr-fum (blue), Zr-stilbene (red), UiO-66 (light blue), and the mesoporous carbon CMK-3 (black). Each data point corresponds to Cl_2 uptake after 20 min of exposure at the indicated pressure.

Dosing with increasing pressures of Cl_2 led Zr-fum to saturate near 400 mbar and Zr-stilbene to saturate near 700 mbar. The resulting increase in mass for Zr-fum (22 wt %) is higher than the theoretical capacity (20 wt %) assuming ~85% linker dichlorination, as observed at lower Cl_2 partial pressures. Zr-stilbene also exhibited an increase in mass (24 wt %) that is higher than the expected change (16 wt %) assuming 100% linker dichlorination. Given that linker-based over-chlorination was not detected by ^1H NMR in other measurements, the apparent over-chlorination of Zr-fum and Zr-stilbene at higher Cl_2 pressures is likely due to the additional non-specific uptake at the Zr nodes or on the glass surface of the capillaries. Notably, the uptake of Cl_2 in Zr-fum was also relatively rapid, as a high uptake (13.4 wt %) was observed after dosing the MOF with 1 bar of Cl_2 for only 5 min (Supporting Information Figures S58−S59).

In order to support that significant irreversible uptake only occurs in materials containing reactive alkene linkages, the mesoporous carbon CMK-3 and the terephthalate-based MOF

https://doi.org/10.1021/acsami.2c17966
ACS Appl. Mater. Interfaces 2022, 14, 53928−53935

UiO-66[44] (which lacks alkene sites in the linker) were subjected to Cl_2 at different pressures. Both materials gained <4 wt % under 998 mbar Cl_2, significantly less than the maximum irreversible uptake of Zr-fum and Zr-stilbene. Consistently, UiO-66 was previously reported to irreversibly gain 1−2 wt % under 1000 mbar Cl_2 due to non-specific chlorination.[20] The non-negligible irreversible Cl_2 uptake of these materials at higher Cl_2 pressures supports that the higher-than-expected uptake of Zr-fum and Zr-stilbene is likely due to non-specific chlorination as well. These findings support that strong, irreversible Cl_2 capture is unique to porous materials containing alkene linkages.

Critically, both Zr-fum and Zr-stilbene irreversibly captured Cl_2 even at lower partial pressures, with Zr-fum, in particular, capturing 9.6 wt % (1.4 mmol/g) of Cl_2 at 169 mbar and Zr-stilbene capturing 6.5 wt % (0.9 mmol/g) of Cl_2 at the same pressure. We hypothesize that the superior gravimetric uptake of Zr-fum compared to Zr-stilbene at lower Cl_2 pressures is due to its lower molecular weight and smaller crystallites. While the molar capacities of the two MOFs should be nearly identical, the lower molecular weight of Zr-fum should lead to higher gravimetric uptake at the same Cl_2 loading. As evidenced by SEM (Supporting Information Figures S7 and S41), the obtained crystallites of Zr-stilbene are also much larger than those of Zr-fum. Despite its larger pores, the larger crystallite size of Zr-stilbene should slow down Cl_2 diffusion to non-surface alkene sites, ultimately leading to a lower observed uptake capacity at low pressures and short Cl_2 exposure times compared to Zr-fum.

CONCLUSIONS

Industrial Cl_2 leaks have continued to cause fatalities and injuries to civilians even as recently as 2022.[45] Part of the ongoing safety challenge is the scarcity of materials that are able to capture oxidizing and corrosive Cl_2 gas. Herein, we have demonstrated that the MOFs Zr-fum and Zr-stilbene enable irreversible Cl_2 capture via dichlorination of their alkene-containing linkers, furnishing the new chlorinated frameworks Cl_2−Zr-fum and Cl_2−Zr-stilbene, respectively. By digestion ^{1}H NMR analysis, up to 85% of Zr-fum could be converted to Cl_2−Zr-fum, while Zr-stilbene could be quantitatively converted to Cl_2−Zr-stilbene. A high level of chemoselectivity for alkene dichlorination was observed in both materials. In addition, low-pressure Cl_2 dosing experiments reveal that these materials are capable of Cl_2 capture at low pressures (<200 mbar) and reach saturation at pressures under 1000 mbar. Both of these materials irreversibly capture Cl_2 significantly better than unfunctionalized UiO-66 and a representative mesoporous carbon. Considering that Zr-MOFs have been widely appended to fabrics already,[46,47] both Zr-fum and Zr-stilbene could function as protective Cl_2 sponges in next-generation PPE. Beyond their application for Cl_2 capture, the linker dichlorination reactions reported herein enable the installation of sp^3-hydridized carbons within MOFs, which is difficult to achieve but can improve the MOF's mechanical properties.[48]

ASSOCIATED CONTENT

Supporting Information

The Supporting Information is available free of charge at https://pubs.acs.org/doi/10.1021/acsami.2c17966.

All synthetic procedures and characterization data (PDF)

AUTHOR INFORMATION

Corresponding Author

Phillip J. Milner − *Department of Chemistry and Chemical Biology, Cornell University, Ithaca, New York 14850, United States*; orcid.org/0000-0002-2618-013X; Email: pjm347@cornell.edu

Authors

Tyler J. Azbell − *Department of Chemistry and Chemical Biology, Cornell University, Ithaca, New York 14850, United States*

Ruth M. Mandel − *Department of Chemistry and Chemical Biology, Cornell University, Ithaca, New York 14850, United States*

Jung-Hoon Lee − *Computational Science Research Center, Korea Institute of Science and Technology (KIST), Seoul 02792, Republic of Korea*

Complete contact information is available at: https://pubs.acs.org/10.1021/acsami.2c17966

Author Contributions

[§]T.J.A. and R.M.M. contributed equally to this work. P.J.M. conceived the project. T.J.A. and R.M.M. synthesized and characterized all MOF samples. J.L. carried out DFT calculations. R.M.M. collected SEM images. The manuscript was written through the contributions of all authors, and all authors approved of the final version.

Funding

Exploring the reactivity of halogens with MOFs was supported by the National Institute of General Medical Sciences of the National Institutes of Health under award number R35GM138165 (T.J.A., R.M.M., and P.J.M.). The content is solely the responsibility of the authors and does not necessarily represent the official views of the National Institutes of Health. T.J.A. thanks Cornell University for financial support through a recruiting fellowship. J.H.L.'s work was supported by the KIST Institutional Program (project no. 2E31801) and the programs of Future Hydrogen Original Technology Development (grant no. 2021M3I3A1083946) and the National Center for Materials Research Data (NCMRD) (2021M3A7C2089739), through the National Research Foundation of Korea (NRF), funded by the Korean government [Ministry of Science and ICT (MSIT)]. Computational resources provided by the KISTI Supercomputing Center (project no. KSC-2020-CRE-0361) are gratefully acknowledged. The construction of the stainless-steel manifold was supported by the ACS Petroleum Research Fund (60378-DNI7). This work made use of the Cornell Center for Materials Research Shared Facilities, which are supported through the NSF MRSEC program (DMR-1719875). ^{1}H NMR data were collected on a Bruker INOVA 500 MHz spectrometer that was purchased with support from the National Science Foundation (CHE-1531632).

Notes

The authors declare the following competing financial interest(s): P.J.M. and R.M.M. are listed as co-inventors on several (provisional) patents related to MOFs. Contributed equally to this work.

■ ACKNOWLEDGMENTS

The authors thank Mary Zick (Cornell University) for her preparation of UiO-66, Jaehwan Kim (Cornell University) for his assembly of the dosing manifold, and both for their helpful contributions during the preparation of the manuscript, as well as Tristan Pitt (Cornell University) for his help with TGA calculations.

■ REFERENCES

(1) Fauvarque, J. The Chlorine Industry. *Pure Appl. Chem.* **1996**, *68*, 1713−1720.
(2) Jones, R.; Wills, B.; Kang, C. Chlorine Gas: An Evolving Hazardous Material Threat and Unconventional Weapon. *West. J. Emerg. Med.* **2010**, *11*, 151−6.
(3) Rahim, M. U.; Gao, X.; Garcia-Perez, M.; Li, Y.; Wu, H. Release of Chlorine during Mallee Bark Pyrolysis. *Energy Fuels* **2013**, *27*, 310−317.
(4) Dhomse, S. S.; Feng, W.; Montzka, S. A.; Hossaini, R.; Keeble, J.; Pyle, J. A.; Daniel, J. S.; Chipperfield, M. P. Delay in Recovery of the Antarctic Ozone Hole from Unexpected CFC-11 Emissions. *Nat. Commun.* **2019**, *10*, 5781.
(5) Saroha, A. K. Safe Handling of Chlorine. *J. Chem. Health Saf.* **2006**, *13*, 5−11.
(6) Smith, E. M.; Plewa, M. J.; Lindell, C. L.; Richardson, S. D.; Mitch, W. A. Comparison of Byproduct Formation in Waters Treated with Chlorine and Iodine: Relevance to Point-of-Use Treatment. *Environ. Sci. Technol.* **2010**, *44*, 8446−8452.
(7) Hu, J. H.; Shi, Q.; Davidovits, P.; Worsnop, D. R.; Zahniser, M. S.; Kolb, C. E. Reactive Uptake of Cl2(g) and Br2(g) by Aqueous Surfaces as a Function of Br- and I- Ion Concentration: The Effect of Chemical Reaction at the Interface. *J. Phys. Chem.* **1995**, *99*, 8768−8776.
(8) Xue, J.; Wen, X.-G.; Zhao, H.; Lv, Z.-P.; Li, F.-X. Chlorine Adsorption of Activated Carbons, Carbon Molecular Sieves and Carbon Nanotubes. *Asian J. Chem.* **2012**, *24*, 5481.
(9) Bevington, J. C.; Ratti, L. Chlorination of 1,4-Polybutadiene. *Polymer* **1975**, *16*, 66−67.
(10) Hahn, S. F.; Dreyfuss, M. P. Novel Polymeric Structures via the Chlorination of Cis-1,4-Polybutadiene in the Presence of Aryl Nucleophiles. *J. Polym. Sci., Part A: Polym. Chem.* **1993**, *31*, 3039−3047.
(11) Rieth, A. J.; Wright, A. M.; Dincă, M. Kinetic stability of metal-organic frameworks for corrosive and coordinating gas capture. *Nat. Rev. Mater.* **2019**, *4*, 708−725.
(12) Li, H.; Li, L.; Lin, R.-B.; Zhou, W.; Zhang, Z.; Xiang, S.; Chen, B. Porous Metal-Organic Frameworks for Gas Storage and Separation: Status and Challenges. *EnergyChem* **2019**, *1*, 100006.
(13) Cheung, Y. H.; Ma, K.; van Leeuwen, H. C.; Wasson, M. C.; Wang, X.; Idrees, K. B.; Gong, W.; Cao, R.; Mahle, J. J.; Islamoglu, T.; Peterson, G. W.; de Koning, M. C.; Farha, J. H.; Farha, O. K. Immobilized Regenerable Active Chlorine within a Zirconium-Based MOF Textile Composite to Eliminate Biological and Chemical Threats. *J. Am. Chem. Soc.* **2021**, *143*, 16777−16785.
(14) Zhou, Y.; Gao, Q.; Zhang, L.; Zhou, Y.; Zhong, Y.; Yu, J.; Liu, J.; Huang, C.; Wang, Y. Combining Two into One: A Dual-Function H5PV2Mo10O40@MOF-808 Composite as a Versatile Decontaminant for Sulfur Mustard and Soman. *Inorg. Chem.* **2020**, *59*, 11595−11605.
(15) Furukawa, H.; Cordova, E.; O'Keeffe, M.; Yaghi, M. The Chemistry and Applications of Metal-Organic Frameworks. *Science* **2013**, *341*, 1230444.
(16) Browe, M. A.; Napolitano, A.; DeCoste, J. B.; Peterson, G. W. Filtration of chlorine and hydrogen chloride gas by engineered UiO-66-NH2 metal-organic framework. *J. Hazard. Mater.* **2017**, *332*, 162−167.
(17) Marshall, R. J.; Griffin, S. L.; Wilson, C.; Forgan, R. S. Stereoselective Halogenation of Integral Unsaturated C-C Bonds in Chemically and Mechanically Robust Zr and Hf MOFs. *Chem.—Eur. J.* **2016**, *22*, 4870−4877.
(18) Marshall, R. J.; Richards, T.; Hobday, C. L.; Murphie, C. F.; Wilson, C.; Moggach, S. A.; Bennett, T. D.; Forgan, R. S. Postsynthetic Bromination of UiO-66 Analogues: Altering Linker Flexibility and Mechanical Compliance. *Dalton Trans.* **2016**, *45*, 4132−4135.
(19) DeCoste, J. B.; Browe, M. A.; Wagner, G. W.; Rossin, J. A.; Peterson, G. W. Removal of chlorine gas by an amine functionalized metal-organic framework via electrophilic aromatic substitution. *Chem. Commun.* **2015**, *51*, 12474−12477.
(20) Tulchinsky, Y.; Hendon, C. H.; Lomachenko, K. A.; Borfecchia, E.; Melot, B. C.; Hudson, M. R.; Tarver, J. D.; Korzyński, M. D.; Stubbs, A. W.; Kagan, J. J.; Lamberti, C.; Brown, C. M.; Dincă, M. Reversible Capture and Release of Cl2 and Br2 with a Redox-Active Metal-Organic Framework. *J. Am. Chem. Soc.* **2017**, *139*, 5992−5997.
(21) Peterson, G. W.; Lu, A. X.; Epps, T. H. Tuning the Morphology and Activity of Electrospun Polystyrene/UiO-66-NH2 Metal-Organic Framework Composites to Enhance Chemical Warfare Agent Removal. *ACS Appl. Mater. Interfaces* **2017**, *9*, 32248−32254.
(22) Britt, D.; Tranchemontagne, D.; Yaghi, O. M. Metal-Organic Frameworks with High Capacity and Selectivity for Harmful Gases. *Proc. Natl. Acad. Sci. U.S.A.* **2008**, *105*, 11623−11627.
(23) Lu, A. X.; McEntee, M.; Browe, M. A.; Hall, M. G.; DeCoste, J. B.; Peterson, G. W. MOFabric: Electrospun Nanofiber Mats from PVDF/UiO-66-NH2 for Chemical Protection and Decontamination. *ACS Appl. Mater. Interfaces* **2017**, *9*, 13632−13636.
(24) Matemb Ma Ntep, T.; Breitzke, H.; Schmolke, L.; Schlüsener, C.; Moll, B.; Millan, S.; Tannert, N.; El Aita, I.; Buntkowsky, G.; Janiak, C. Facile in Situ Halogen Functionalization via Triple-Bond Hydrohalogenation: Enhancing Sorption Capacities through Halogenation to Halofumarate-Based Zr(IV)-Metal-Organic Frameworks. *Chem. Mater.* **2019**, *31*, 8629−8638.
(25) Walshe, C. A.; Thom, A. J. R.; Wilson, C.; Ling, S.; Forgan, R. S. Controlling the Flexibility of MIL-88A(Sc) Through Synthetic Optimisation and Postsynthetic Halogenation. *Chem.—Eur. J.* **2022**, *28*, No. e202201364.
(26) Peterson, G. W.; Destefano, M. R.; Garibay, S. J.; Ploskonka, A.; McEntee, M.; Hall, M.; Karwacki, C. J.; Hupp, J. T.; Farha, O. K. Optimizing Toxic Chemical Removal through Defect-Induced UiO-66-NH 2 Metal-Organic Framework. *Chem.–Eur. J.* **2017**, *23*, 15913−15916.
(27) Wang, Z.; Bilegsaikhan, A.; Jerozal, R. T.; Pitt, T. A.; Milner, P. J. Evaluating the Robustness of Metal-Organic Frameworks for Synthetic Chemistry. *ACS Appl. Mater. Interfaces* **2021**, *13*, 17517−17531.
(28) Chen, F. E.; Mandel, R. M.; Woods, J. J.; Lee, J.-H.; Kim, J.; Hsu, J. H.; Fuentes-Rivera, J. J.; Wilson, J. J.; Milner, P. J. Biocompatible metal-organic frameworks for the storage and therapeutic delivery of hydrogen sulfide. *Chem. Sci.* **2021**, *12*, 7848−7857.
(29) Chen, Y.; Zhang, X.; Ma, K.; Chen, Z.; Wang, X.; Knapp, J.; Alayoglu, S.; Wang, F.; Xia, Q.; Li, Z.; Islamoglu, T.; Farha, O. K. Zirconium-Based Metal-Organic Framework with 9-Connected Nodes for Ammonia Capture. *ACS Appl. Nano Mater.* **2019**, *2*, 6098−6102.
(30) Jasuja, H.; Peterson, G. W.; Decoste, J. B.; Browe, M. A.; Walton, K. S. Evaluation of MOFs for Air Purification and Air Quality Control Applications: Ammonia Removal from Air. *Chem. Eng. Sci.* **2015**, *124*, 118−124.
(31) Marshall, R. J.; Griffin, S. L.; Wilson, C.; Forgan, R. S. Single-Crystal to Single-Crystal Mechanical Contraction of Metal-Organic Frameworks through Stereoselective Postsynthetic Bromination. *J. Am. Chem. Soc.* **2015**, *137*, 9527−9530.
(32) Furukawa, H.; Gándara, F.; Zhang, Y.-B.; Jiang, J.; Queen, W. L.; Hudson, M. R.; Yaghi, O. M. Water Adsorption in Porous Metal-Organic Frameworks and Related Materials. *J. Am. Chem. Soc.* **2014**, *136*, 4369−4381.

(33) Ahmad, K.; Nazir, M. A.; Qureshi, A. K.; Hussain, E.; Najam, T.; Javed, M. S.; Shah, S. S. A.; Tufail, M. K.; Hussain, S.; Khan, N. A.; Shah, H.-R.; Ashfaq, M. Engineering of Zirconium Based Metal-Organic Frameworks (Zr-MOFs) as Efficient Adsorbents. *Mater. Sci. Eng. B* **2020**, *262*, 114766.
(34) Reinsch, H.; Waitschat, S.; Chavan, S. M.; Lillerud, K. P.; Stock, N. A Facile "Green" Route for Scalable Batch Production and Continuous Synthesis of Zirconium MOFs. *Eur. J. Inorg. Chem.* **2016**, *2016*, 4490−4498.
(35) Cresswell, A. J.; Eey, S. T.-C.; Denmark, S. E. Catalytic, Stereospecific Syn-Dichlorination of Alkenes. *Nat. Chem.* **2015**, *7*, 146−152.
(36) Atterberg, A.; Widman, O. Neue Chlornaphtaline. *Ber. Dtsch. Chem. Ges.* **1877**, *10*, 1841−1844.
(37) Marshall, R. J.; Hobday, C. L.; Murphie, C. F.; Griffin, S. L.; Morrison, C. A.; Moggach, S. A.; Forgan, R. S. Amino acids as highly efficient modulators for single crystals of zirconium and hafnium metal-organic frameworks. *J. Mater. Chem. A* **2016**, *4*, 6955−6963.
(38) Øien-Ødegaard, S.; Lillerud, K. Twinning in Zr-Based Metal-Organic Framework Crystals. *Chemistry* **2020**, *2*, 777−786.
(39) Wang, S.; Xhaferaj, N.; Wahiduzzaman, M.; Oyekan, K.; Li, X.; Wei, K.; Zheng, B.; Tissot, A.; Marrot, J.; Shepard, W.; Martineau-Corcos, C.; Filinchuk, Y.; Tan, K.; Maurin, G.; Serre, C. Engineering Structural Dynamics of Zirconium Metal-Organic Frameworks Based on Natural C4 Linkers. *J. Am. Chem. Soc.* **2019**, *141*, 17207−17216.
(40) Xu, X.; Yang, F.; Chen, S.-L.; He, J.; Xu, Y.; Wei, W. Dynamic Behaviours of a Rationally Prepared Flexible MOF by Postsynthetic Modification of Ligand Struts. *Chem. Commun.* **2017**, *53*, 3220−3223.
(41) Ruasse, M. F. Bromonium Ions or .Beta.-Bromocarbocations in Olefin Bromination. A Kinetic Approach to Product Selectivities. *Acc. Chem. Res.* **1990**, *23*, 87−93.
(42) De la Mare, P. B. Pathways in Electrophilic Aromatic Substitutions. Cyclohexadienes and Related Compounds as Intermediates in Halogenation. *Acc. Chem. Res.* **1974**, *7*, 361−368.
(43) Jeong, S.; Milner, P. J.; Wan, L. F.; Liu, Y.-S.; Oktawiec, J.; Zaia, E. W.; Forse, A. C.; Leick, N.; Gennett, T.; Guo, J.; Prendergast, D.; Long, J. R.; Urban, J. J. Runaway Carbon Dioxide Conversion Leads to Enhanced Uptake in a Nanohybrid Form of Porous Magnesium Borohydride. *Adv. Mater.* **2019**, *31*, 1904252.
(44) Cavka, J. H.; Jakobsen, S.; Olsbye, U.; Guillou, N.; Lamberti, C.; Bordiga, S.; Lillerud, K. P. A New Zirconium Inorganic Building Brick Forming Metal Organic Frameworks with Exceptional Stability. *J. Am. Chem. Soc.* **2008**, *130*, 13850−13851.
(45) Pannett, R. *Chlorine Gas Leak at Port in Jordan Kills at Least 13, Injures Hundreds*; The Washington Post, June 28, 2022.
(46) Gouma, V.; Pournara, A. D.; Manos, M. J.; Giokas, D. L. Fabric Phase Sorpitive Extraction and Passive Sampling of Ultraviolet Filters from Natural Waters Using a Zirconium Metal Organic Framework-Cotton Composite. *J. Chromatogr. A* **2022**, *1670*, 462945.
(47) Rezaee, R.; Montazer, M.; Mianehro, A.; Mahmoudirad, M. Biomedical Applicable Cellulose Fabric Modified with Zirconium-Based Metal-Organic Frameworks (Zr-MOFs). *Starch* **2021**, *73*, 2100120.
(48) Pallach, R.; Keupp, J.; Terlinden, K.; Frentzel-Beyme, L.; Kloß, M.; Machalica, A.; Kotschy, J.; Vasa, S. K.; Chater, P. A.; Sternemann, C.; Wharmby, M. T.; Linser, R.; Schmid, R.; Henke, S. Frustrated Flexibility in Metal-Organic Frameworks. *Nat. Commun.* **2021**, *12*, 4097.

https://doi.org/10.1021/acsami.2c17966
ACS Appl. Mater. Interfaces 2022, 14, 53928−53935